

High endothelial venule-like vessels and lymphocyte recruitment in testicular seminoma

Yasuhiro Sakai¹, Hitomi Hoshino², Riko Kitazawa³, and Motohiro Kobayashi²

¹Department of Molecular Pathology, Shinshu University Graduate School of Medicine, Matsumoto, Japan; ²Division of Tumor Pathology, Department of Pathological Sciences, Faculty of Medical Sciences, University of Fukui, Eiheiji, Japan; ³Division of Molecular Pathology, Ehime University Graduate School of Medicine, Toon, Japan

Correspondence: Motohiro Kobayashi, Division of Tumor Pathology, Department of Pathological Sciences, Faculty of Medical Sciences, University of Fukui, 23-3 Matsuoka-Shimoaizuki, Eiheiji, Fukui 910-1193, Japan

E-mail address: motokoba@u-fukui.ac.jp

TEL: +81-776-61-8319 / FAX: +81-776-61-8103

SUMMARY

Seminoma, the most common testicular malignant neoplasm, originates from germ cells and is characterized by the presence of numerous tumor-infiltrating lymphocytes (TILs).

Although it is widely accepted that TILs function in surveillance and cytotoxicity in various tumors including seminoma, detailed mechanisms governing TIL recruitment are not fully understood. It has been shown that high endothelial venule (HEV)-like vessels are induced in inflamed and neoplastic tissues and contribute to lymphocyte recruitment in a manner similar to the way physiological lymphocyte homing occurs in secondary lymphoid organs.

Here, we report that HEV-like vessels, which express MECA-79⁺ 6-sulfo sialyl Lewis X-capped structures, are induced in TIL aggregates in seminoma, and that such vessels potentially recruit circulating lymphocytes, since an E-selectin•IgM chimera binds these vessels in a calcium-dependent manner. These HEV-like vessels express intercellular adhesion molecule 1 (ICAM-1), but not vascular cell adhesion molecule 1 (VCAM-1) or mucosal addressin cell adhesion molecule 1 (MAdCAM-1), which likely contributes to lymphocyte firm attachment. We also found that the number of T cells attached to the luminal surface of HEV-like vessels was greater than the number of B cells ($p < 0.0001$).

Interestingly, while CD8⁺ cytotoxic T lymphocytes (CTLs) attached to the lumen of HEV-like

vessels were scarcely detected, significant numbers of proliferative CTLs were observed outside vessels. These histological findings strongly suggest that TILs, particularly T cells, are recruited to seminoma tissues via HEV-like vessels, and that tumor-infiltrating CTLs then undergo proliferation after transmigration through HEV-like vessels in testicular seminoma.

INTRODUCTION

Seminoma, also called pure seminoma or classical seminoma, is the most common malignant testicular tumor originating from germ cells in the seminiferous tubules. Histologically, it is characterized by a so-called “two-cell pattern” composed of 1) uniformly large-sized tumor epithelial cells with glycogen-rich clear cytoplasm, which form sheet-like nests, and 2) tumor-infiltrating lymphocytes (TILs), which form lymphoid aggregates (Nakanoma *et al.*, 1992). It is widely accepted that TILs play an important role in surveillance and inhibition of tumor growth. In fact, it is reported that, in certain tumors such as breast, colorectal, and ovarian carcinomas, variants exhibiting a large number of TILs have more favorable clinical outcomes (Naito *et al.*, 1998; Zhang *et al.*, 2003; Pagès *et al.*, 2005; Sato *et al.*, 2005; Galon *et al.*, 2006; Disis, 2010). In the case of seminoma, a relatively low TIL count is reportedly associated with increased risk of relapse in patients with stage I disease (Parker *et al.*, 2002). Thus, to understand tumor immunity, it is important to clarify the origin of TILs.

We hypothesized that TILs in seminoma are recruited via high endothelial venule (HEV)-like vessels. Unlike common venules, which exhibit flat endothelial cells, HEVs are composed of plump cuboidal endothelial cells found in secondary lymphoid organs (De Bruyn & Cho, 1990). There, they have been proposed to play an important role in

lymphocyte “homing”, a multistep process mediated by sequential adhesive interactions between circulating lymphocytes and HEVs (Butcher & Picker, 1996; Girard *et al.*, 2012).

In the initial step, glycoproteins decorated with 6-sulfo sialyl Lewis X (sLeX) on the HEV luminal surface form a weak bond with L-selectin expressed on circulating lymphocytes, causing “tethering and rolling” of lymphocytes (Paavonen & Renkonen, 1992; Sawada *et al.*, 1993; Mitsuoka *et al.*, 1997). A monoclonal antibody MECA-79 has been widely used for a marker of HEVs, since this antibody recognizes 6-sulfo *N*-acetyllactosamine attached to extended core 1 *O*-glycans, which constitutes one of 6-sulfo sLeX-capped L-selectin ligand carbohydrates (Streeter *et al.*, 1988a; Yeh *et al.*, 2001). After lymphocyte activation by various cytokines, subsequent “arrest (sticking)” step is mediated by a firm adhesive interaction between cell adhesion molecules of the immunoglobulin superfamily expressed on HEVs and integrins expressed on lymphocytes; the former include intercellular adhesion molecule 1 (ICAM-1), vascular cell adhesion molecule 1 (VCAM-1), and mucosal addressin cell adhesion molecule 1 (MAdCAM-1), which bind to $\alpha_L\beta_2$, $\alpha_4\beta_1$, and $\alpha_4\beta_7$ integrins, respectively (Rothlein *et al.*, 1986; Schwartz *et al.*, 1990; Berlin *et al.*, 1993; Jones *et al.*, 1994; Hoshino *et al.*, 2011). Lymphocytes then “crawl” along the lumen of HEVs, “transmigrate” through the appropriate sites of HEVs, “accumulate” transitionally in a

pocket-like structure below HEVs, and finally, transfer and position to the appropriate zones of lymph nodes (Girard *et al.*, 2012).

In various non-lymphoid organs under chronic inflammatory conditions such as chronic *Helicobacter pylori* gastritis, inflammatory bowel disease, and autoimmune pancreatitis (Kobayashi *et al.*, 2004 & 2009; Suzawa *et al.*, 2007; Maruyama *et al.*, 2013), venules morphologically and immunohistochemically similar to HEVs (HEV-like vessels) appear at inflamed sites, suggesting that these vessels function in disease pathogenesis.

HEV-like vessels are also observed in and around various neoplastic tissues (Tanaka *et al.*, 1992; Kobayashi *et al.*, 2011; Martinet *et al.*, 2011 & 2012; Ohya *et al.*, 2013); however, the appearance of HEV-like vessels in seminoma tissues has not been reported in the literature.

Here we show that HEV-like vessels appear in testicular seminoma and that these vessels potentially recruit circulating lymphocytes. We also show that lymphocytes, particularly T cells, attached to the luminal surface of HEV-like vessels, and cytotoxic T lymphocytes (CTLs) proliferate outside the vessels. These findings collectively indicate that both 1) TILs recruited via HEV-like vessels and 2) CTLs proliferated after recruitment via HEV-like vessels contribute to the histogenesis of testicular seminoma.

MATERIALS AND METHODS

Human histological samples

Formalin-fixed, paraffin-embedded tissue blocks of surgical specimens of testicular seminoma ($n = 26$) were retrieved from the pathological archives of the Department of Laboratory Medicine, Shinshu University Hospital. Clinical characteristics of the patients are summarized in Table 1. The analysis of testicular seminoma tissues was approved by the Ethics Committee of Shinshu University School of Medicine.

Immunohistochemistry and immunofluorescence

Conventional immunostaining with MECA-79 (recognizing 6-sulfo *N*-acetylactosamine attached to extended core 1 *O*-glycans; rat IgM, BD Pharmingen, San Diego, CA; Streeter *et al.*, 1988a; Yeh *et al.*, 2001) and HECA-452 (recognizing sLeX attached to both *N*- and *O*-glycans; rat IgM, BD Pharmingen; Duijvestijn *et al.*, 1988) was performed by an indirect method.

Triple immunostaining for CD20 and CD79 α (for B cells), CD3 (for T cells), and MECA-79 (for HEV-like vessels) was performed as described previously (Suzawa *et al.*, 2007) with modifications. Briefly, after deparaffinization, rehydration, antigen retrieval and

blocking, sections were incubated for 60 min with a cocktail of L26 (directed to CD20, mouse IgG2 α , Dako, Glostrup, Denmark) and JCB117 (directed to CD79 α , mouse IgG1 κ , Dako) followed by a 30-min incubation with alkaline phosphatase (AP)-conjugated EnVision (Dako). The color reaction was developed using Vulcan Fast Red Chromogen Kit 2 (Biocare Medical, Concord, CA). To dissociate antibodies, sections were boiled for 10 min in 6.3 mM Tris buffer (pH 8.6) containing 1 mM EDTA. Sections were then incubated with rabbit anti-human CD3 polyclonal antibody (Dako) for 60 min followed by a 30-min incubation with AP-conjugated EnVision. The color reaction was developed with Ferangi Blue Chromogen Kit 2 (Biocare Medical). After dissociating the antibodies again, endogenous peroxidase activity was quenched by soaking sections in 3% H₂O₂ solution for 30 min. Sections were then incubated with MECA-79 at 4°C overnight followed by a 30-min incubation with horseradish peroxidase (HRP)-conjugated rabbit anti-rat immunoglobulins (Dako). The color reaction was developed with 3,3'-diaminobenzidine (DAB). Sections were mounted with Glycergel mounting medium (Dako).

Double immunostaining for CD8 and either MECA-79 or Ki-67 was carried out in a similar fashion. In the first staining, C8/114B (directed to CD8, mouse IgG1 κ , Dako) and HRP-conjugated EnVision+ (Dako) were used, and the color reaction was developed with a

VECTOR VIP Peroxidase Substrate Kit (Vector Laboratories, Burlingame, CA). In the second staining, a combination of either MECA-79 and HRP-conjugated rabbit anti-rat immunoglobulins, or MIB-1 (directed to Ki-67, mouse IgG1 κ , Dako) and HRP-conjugated anti-mouse EnVision+ was used, and the color reaction was developed with DAB. Sections were dehydrated, cleaned, and mounted with an insoluble mounting medium.

Double immunofluorescence for MECA-79 and either with anti-ICAM-1 (rabbit IgG polyclonal, Atlas Antibodies, Stockholm, Sweden), EPR5047 (directed to VCAM-1, rabbit IgG, Abcam, Cambridge, UK), or 17F5 (directed to MAdCAM-1, mouse IgG1, Abcam) or for C8/114B and anti-human CD3 monoclonal antibody was undertaken as described previously (Shimojo *et al.*, 2011) using appropriate secondary antibodies.

Quantification of HEV-like vessels and CD3⁺, CD20/79 α ⁺, and CD8⁺ lymphocytes

The number of HEV-like vessels in tissue sections was determined by MECA-79⁺ immunostaining. The number of CD3⁺ T cells, CD20/79 α ⁺ B cells, and CD8⁺ CTLs attached to the luminal surface of those vessels was also counted in corresponding sections. From these numbers, the number of MECA-79⁺ HEV-like vessels/cm² and the mean number of each lymphocyte subset attached to a single HEV-like vessel were calculated, as described

previously (Ohya *et al.*, 2013). Additionally, the number of CD3⁺ T cells/high power field (HPF) in immunostained tissue sections was determined by counting CD3⁺ cells in 5 HPFs of the most prominent appearance of TILs. The above evaluation was performed using a BX-51 light microscope (Olympus, Tokyo, Japan) at a magnification of x200.

In vitro E-selectin•IgM chimera binding assay

An E-selectin•IgM chimera was obtained from the culture medium of COS-1 cells transiently transfected with pcDNA1.1-E-selectin•IgM, and an E-selectin•IgM binding assay was carried out as described (Kobayashi *et al.*, 2004). Briefly, after deparaffinization, rehydration, and quenching endogenous peroxidase activity, sections were blocked with Dulbecco's Modified Eagle's Medium (DMEM; Life Technologies, Carlsbad, CA) supplemented with 10% fetal bovine serum (FBS; HyClone, Logan, UT). Sections were incubated with the E-selectin•IgM chimera for 60 min and then with HRP-conjugated goat anti-human IgM antibody (Pierce Biotechnology, Rockford, IL) diluted with DMEM supplemented with FBS. The color reaction was developed with DAB. Negative control experiments were done by substituting DMEM with DMEM supplemented with 10 mM EDTA to chelate divalent cations.

Statistical analysis

All statistical analyses were performed using GraphPad Prism 6 software (GraphPad Software, La Jolla, CA). Difference of the number of MECA-79⁺ HEV-like vessels/cm² among groups categorized by pT classification (pT1, pT2, and pT3/4), S classification (S0, S1, and S2), and stage (stage I, II, and III) was analyzed by the Kruskal-Wallis test, while that between groups with or without regional lymph node metastasis was done by the Mann-Whitney *U*-test.

Difference between the number of T and B cells attached to the luminal surface of HEV-like vessels was analyzed by Welch's *t*-test. Correlations between the number of MECA-79⁺ HEV-like vessels/cm² and either 1) age or 2) the number of CD3⁺ T cells/HPF were analyzed by Spearman's rank correlation coefficient. In all tests, *p* values less than 0.05 were considered significant.

RESULTS

Appearance of MECA-79⁺ HEV-like vessels in TIL aggregates in seminoma

Hematoxylin and eosin-stained tissue sections of seminoma exhibited characteristic histological features, namely, infiltrated lymphocytes forming lymphoid aggregates among tumor epithelial cell nests (Fig. 1, left upper panel) in all the cases examined. In and around such TIL aggregates, we observed venules morphologically similar to HEVs, whose luminal surface was positively immunostained with MECA-79 antibody in 24 out of 26 cases (92.3%), and lymphocytes were attached to the luminal surface of these vessels (Fig. 1, left lower and middle panels). The mean number of MECA-79⁺ HEV-like vessels/cm² was $3.2 \pm 5.6/\text{cm}^2$ on tissue specimens. There were no statistically significant associations between the number of MECA-79⁺ HEV-like vessels/cm² and clinical characteristics including age ($r = 0.3673$, $p = 0.0649$), pT classification ($p = 0.0895$), S classification ($p = 0.1046$), stage ($p = 0.3100$), and the presence or absence of regional lymph node metastasis ($p = 0.5035$).

Expression of lymphocyte homing-related adhesion molecules on HEV-like vessels in seminoma

To determine whether the glycostructure expressed on HEV-like vessels in seminoma is identical to that on HEVs in secondary lymphoid organs, we carried out immunostaining with

HECA-452 antibody in addition to MECA-79 antibody. As shown in Fig. 1 (middle and right panels), both MECA-79 and HECA-452 decorated the same HEV-like vessels in seminoma, indicating the presence of 6-sulfo sLeX attached to extended core 1 *O*-glycans.

To determine whether such *O*-glycans potentially function as an L-selectin ligand, we carried out an *in vitro* binding assay using L- and E-selectin•IgM chimeras as a functional probe for

6-sulfo sLeX and non-sulfated sLeX, respectively (Uchimura *et al.*, 2005). The

E-selectin•IgM chimera bound to HEV-like vessels in the presence of calcium (Fig. 2, left panel), and such binding was completely abrogated by addition of EDTA (Fig. 2, right panel).

L-selectin•IgM chimera did not show such bindings (data not shown). We also carried out immunofluorescence assays for cell adhesion molecules functioning in the arrest step of

lymphocyte homing. As shown in Fig. 3, MECA-79⁺ HEV-like vessels were immunostained with ICAM-1 but not with VCAM-1 or MAdCAM-1. These findings indicate that HEV-like

vessels in seminoma potentially recruit circulating lymphocytes, and that ICAM-1 likely functions in the arrest step of lymphocyte recruitment.

Recruitment and subsequent proliferation of CD8⁺ T cells in seminoma

To define predominant lymphocyte subsets recruited via HEV-like vessels in seminoma, we

undertook triple immunostaining for HEV-like vessels together with markers of T and B cells in the same tissue sections. As shown in Fig. 4A, most TILs were shown to be CD3⁺ T cells (shown in blue), while some CD20/79 α ⁺ B cells (shown in red) were distributed sporadically to form lymphoid follicles. The mean number of such CD3⁺ T cells was 780.8 \pm 318.2/high power field (HPF). Interestingly, most HEV-like vessels were located in the T-cell zone (Figs. 6B and C), although there was no significant correlation between the density of CD3⁺ T cells and HEV-like vessels ($r = 0.3758$, $p = 0.0585$). We also found that the number of CD3⁺ T cells attached to the luminal surface of HEV-like vessels was greater than that of CD20/79 α ⁺ B cells ($p < 0.0001$, Figs. 4C and 5). Moreover, while most T cells infiltrating seminoma tissues were CD8⁺ CTLs (Fig. 6), we could barely detect CD8⁺ CTLs attached to the luminal surface of HEV-like vessels (Figs. 5 and 7A). Double immunostaining demonstrated that a large number of CD8⁺ CTLs infiltrating seminoma were also Ki-67-positive (Fig. 7B). Overall, these findings strongly suggest that most CD8⁺ CTLs that have infiltrated seminoma originate from naïve T cells recruited via HEV-like vessels and that such naïve T cells then proliferate in extravascular sites.

DISCUSSION

The present study demonstrates the appearance of HEV-like vessels in seminoma and shows that such vessels express 6-sulfo sLeX attached to extended core 1 *O*-glycans, which function in the initial step of lymphocyte homing. It has been reported that lymphocytes are recruited to target tissues via MECA-79⁺ HEV-like vessels not only in chronic inflammatory diseases but also in some neoplastic diseases (Tanaka *et al.*, 1992; Kobayashi *et al.*, 2004, 2009 & 2011; Suzawa *et al.*, 2007; Martinet *et al.*, 2011 & 2012; Maruyama *et al.*, 2013; Ohya *et al.*, 2013). In the latter, those vessels may function to increase opportunities for lymphocytes to encounter cognate antigens (Butcher & Picker, 1996). Seminoma cells express melanoma-associated gene (MAGE) antigens, which are types of cancer/testis antigens, which can be targeted by the host tumor immunity (Grobholz *et al.*, 2000; Hadrup *et al.*, 2006; Bode *et al.*, 2011). It is tempting to speculate that HEV-like vessels in seminoma help lymphocytes efficiently recognize such tumor-associated antigens.

Intriguingly, in the present study, L-selectin•IgM chimera did not bind to MECA-79⁺ HEV-like vessels in seminoma (data not shown) while E-selectin•IgM did. Previously, we demonstrated L-selectin•IgM chimera bindings to HEV-like vessels induced in chronic *Helicobacter pylori* gastritis (Kobayashi *et al.*, 2004) and ulcerative colitis (Suzawa *et al.*, 2007); however, the signal intensity was much weaker compared to that seen in original

HEVs in secondary lymphoid organs (Kobayashi *et al.*, 2004). Thus, we hypothesize that the degree of *N*-acetylglucosamine (GlcNAc)-6-*O*-sulfation in the sLeX moiety expressed on HEV-like vessels in seminoma may be much lower than that seen not only in original HEVs in secondary lymphoid organs but also in HEV-like vessels in chronic *Helicobacter pylori* gastritis and ulcerative colitis. The degree of GlcNAc-6-*O*-sulfation may regulate the number of lymphocytes transmigrated via HEV-like vessels in order to prevent excess lymphocyte recruitment. Another possibility is that an L-selectin-independent mechanism might play a role in the lymphocyte recruitment in seminoma.

We also found that ICAM-1 but not VCAM-1 or MAdCAM-1 is expressed on HEV-like vessels in seminoma. All three cell adhesion molecules play an important role in the arrest step of lymphocyte homing; however, their distribution and activities differ.

ICAM-1 is constitutively expressed on endothelial cells as well as thymic epithelial cells, macrophages, and stimulated lymphocytes (Dustin *et al.*, 1986; Padros *et al.*, 1992).

VCAM-1 is minimally expressed on endothelial cells, but its expression is upregulated in inflammatory status (Carlos *et al.*, 1990). On the other hand, expression of MAdCAM-1 is restricted to HEVs in mucosa-associated lymphoid tissue (MALT) (Streeter *et al.*, 1988b).

Although some studies show induction of VCAM-1 expression on endothelial cells

constituting conventional venules but not those constituting HEV-like vessels under inflammatory conditions (Chin *et al.*, 1997; Iiyama *et al.*, 1999), VCAM-1 expression is only occasionally observed in HEVs in secondary lymphoid organs (Tanaka *et al.*, 1994). This observation is consistent with our results.

Here, we found that the number of T cells attached to the luminal surface of HEV-like vessels in seminoma was greater than that of B cells. The selectivity of lymphocyte subsets recruited via HEVs depends on a chemokine-mediated activation step. C-C motif chemokine ligand 19 (CCL19) and CCL21 stimulate C-C chemokine receptor 7 (CCR7)-positive central memory T cells to promote T-cell adhesion to HEVs (Yoshida *et al.*, 1998; Bromley *et al.*, 2005), while C-X-C motif chemokine 13 (CXCL13) functions as a B-cell chemoattractant through its receptor C-X-C chemokine receptor 5 (CXCR5) (Gunn *et al.*, 1998). These mechanisms likely play a role in preferential recruitment of T cells via HEV-like vessels in seminoma as well. In present study, we found that while CD8⁺ CTLs were rarely attached to the luminal surface of HEV-like vessels in seminoma, many CD8⁺ CTLs in extravascular sites were Ki-67-positive, indicating that they proliferate after recruitment and transmigration via HEV-like vessels. In line with this finding, others have reported that CD107a⁺ granzyme B⁺ activated CTLs in seminoma are clonally expanded

based on analysis of T-cell receptor clonotypes (Hadrup *et al.*, 2006). Thus, it is reasonable to conclude that antigen-presentation and subsequent lymphocyte activation occurs near tumor cells and that only T cells expressing cognate receptors for tumor antigens proliferate.

In this study, we analyzed the relation between the density of HEV-like vessels and either the infiltrating T-cell density or several clinical characteristics; however, no correlation was found in any combinations. The former is reasonable because there are many CD8⁺ Ki-67⁺ CTLs expanding in extravascular sites. In the latter, with respect to breast cancer, Martinet *et al.* (2011) reported that the density of HEV-like vessels was correlated statistically with survival rate, but not with clinical characteristics such as tumor size and grading. Testicular seminoma tends to be the same as breast cancer except for survival rate because it is one of the most treatable and curable cancers with highest survival rate (von der Maase *et al.*, 1993).

Several reports suggest that cytokines such as tumor necrosis factor (TNF)- α , lymphotoxin (LT)- α , and LT- $\alpha\beta$ stimulate GlcNAc-6-*O*-sulfation in the sLeX moiety by increasing the expression levels of GlcNAc-6-*O*-sulfotransferase 2 (GlcNAc6ST-2) (Pablos *et al.*, 2005). These cytokines also reportedly increase the expression level of ICAM-1 on HEVs (Poerber *et al.*, 1986; Wellicome *et al.*, 1990; Schrama *et al.*, 2001). It is tempting to

speculate that these HEV-inducing cytokines may impact TIL migration and consequent characteristic histogenesis of seminoma. Further studies are required to evaluate expression of HEV-inducing cytokines to reveal their direct effect in induction of HEV-like vessels in seminoma.

ACKNOWLEDGEMENTS

We thank Dr. Jun Nakayama for encouragement, Ms. Yoshiko Sato for technical assistance, and Dr. Elise Lamar for critical reading of the manuscript. Part of the work was presented at the Annual Meeting of the Japanese Society of Pathology (JSP) held in Sapporo, June 6-8, 2013. Yasuhiro Sakai was the winner of the Best Poster Award at the JSP Conference for Investigative Pathology, held in Kobe, August 2-3, 2013. This study was supported in part by a Grant-in-Aid for Scientific Research 24590410 from the Japan Society for the Promotion of Science (to MK).

AUTHORS' CONTRIBUTIONS

YS designed and performed the research, analyzed the data, and wrote the paper; HH and RK performed the research; and MK conceived and designed the research, analyzed the data, and wrote the paper.

COMPETING INTERESTS

The authors have declared no competing interests.

REFERENCES

Berlin C, Berg EL, Briskin MJ, Andrew DP, Kilshaw PJ, Holzmann B *et al.* (1993) $\alpha 4\beta 7$

integrin mediates lymphocyte binding to the mucosal vascular addressin MAdCAM-1.

Cell 74: 185-195.

Bode PK, Barghorn A, Fritzsche FR, Riener MO, Kristiansen G, Knuth A *et al.* (2011)

MAGEC2 is a sensitive and novel marker for seminoma: a tissue microarray analysis

of 325 testicular germ cell tumors. *Mod Pathol* 24: 829-835.

Bromley SK, Thomas SY & Luster AD. (2005) Chemokine receptor CCR7 guides T cell exit

from peripheral tissues and entry into afferent lymphatics. *Nat Immunol* 6: 895-901.

Butcher EC & Picker LJ. (1996) Lymphocyte homing and homeostasis. *Science* 572: 60-66.

Carlos TM, Schwartz BR, Kovach NL, Yee E, Rosa M, Osborn L *et al.* (1990) Vascular cell

adhesion molecule-1 mediates lymphocyte adherence to cytokine-activated cultured

human endothelial cells. *Blood* 76: 965-970.

Chin JE, Hatfield CA, Winterrowd GE, Brashler JR, Vonderfecht SL, Fidler SF *et al.* (1997)

Airway recruitment of leukocytes in mice is dependent on $\alpha 4$ -integrins and vascular

cell adhesion molecule-1. *Am J Physiol* 272: L219-229.

De Bruyn PP & Cho Y. (1990) Structure and function of high endothelial postcapillary

venules in lymphocyte circulation. *Curr Top Pathol* 84: 85-101.

Disis ML. (2010) Immune regulation of cancer. *J Clin Oncol* 28: 4531-4538.

Duijvestijn AM, Horst E, Pals ST, Rouse BN, Steere AC, Picker LJ *et al.* (1988) High endothelial differentiation in human lymphoid and inflammatory tissues defined by monoclonal antibody HECA-452. *Am J Pathol* 130: 147-155.

Dustin ML, Rothlein R, Bhan AK, Dinarello CA & Springer TA. (1986) Induction by IL 1 and interferon-gamma: tissue distribution, biochemistry, and function of a natural adherence molecule (ICAM-1). *J Immunol* 137: 245-254.

Galon J, Costes A, Sanchez-Cabo F, Kirilovsky A, Mlecnik B, Lagorce-Pagès C *et al.* (2006) Type, density, and location of immune cells within human colorectal tumors predict clinical outcome. *Science* 313: 1960-1964.

Girard JP, Moussion C & Förster R. (2012) HEVs, lymphatics and homeostatic immune cell trafficking in lymph nodes. *Nat Rev Immunol* 12: 762-773.

Grobholz R, Verbeke CS, Schleger C, Köhrmann KU, Hein B, Wolf G *et al.* (2000) Expression of MAGE antigens and analysis of the inflammatory T-cell infiltrate in human seminoma. *Urol Res* 28: 398-403.

Gunn MD, Ngo VN, Ansel KM, Ekland EH, Cyster JG & Williams LT. (1998) A B-cell-homing chemokine made in lymphoid follicles activates Burkitt's lymphoma

receptor-1. *Nature* 391: 799-803.

Hadrup SR, Braendstrup O, Jacobsen GK, Mortensen S, Pedersen LØ, Seremet T *et al.* (2006)

Tumor infiltrating lymphocytes in seminoma lesions comprise clonally expanded cytotoxic T cells. *Int J Cancer* 119: 831-838.

Hoshino H, Kobayashi M, Mitoma J, Sato Y, Fukuda M & Nakayama J. (2011) An integrin

$\alpha 4\beta 7$ -IgG heterodimeric chimera binds to MAdCAM-1 on high endothelial venules in gut-associated lymphoid tissue. *J Histochem Cytochem* 59: 572-583.

Iiyama K, Hajra L, Iiyama M, Li H, DiChiara M, Medoff BD *et al.* (1999) Patterns of

vascular cell adhesion molecule-1 and intercellular adhesion molecule-1 expression in rabbit and mouse atherosclerotic lesions and at sites predisposed to lesion formation.

Circ Res 85: 199-207.

Jones DA, McIntire LV, Smith CW & Picker LJ. (1994) A two-step adhesion cascade for T

cell/endothelial cell interactions under flow conditions. *Clin Invest* 94: 2443-2450.

Kobayashi M, Mitoma J, Nakamura N, Katsuyama T, Nakayama J & Fukuda M. (2004)

Induction of peripheral lymph node addressin in human gastric mucosa infected by *Helicobacter pylori*. *Proc Natl Acad Sci U S A* 101: 17807-17812.

Kobayashi M, Hoshino H, Masumoto J, Fukushima M, Suzawa K, Kageyama S *et al.* (2009)

GlcNAc6ST-1-mediated decoration of MAdCAM-1 protein with L-selectin ligand carbohydrates directs disease activity of ulcerative colitis. *Inflamm Bowel Dis* 15: 697-706.

Kobayashi M, Mitoma J, Hoshino H, Yu SY, Shimojo Y, Suzawa K *et al.* (2011) Prominent expression of sialyl Lewis X-capped core 2-branched *O*-glycans on high endothelial venule-like vessels in gastric MALT lymphoma. *J Pathol* 224: 67-77.

Martinet L, Garrido I, Filleron T, Le Guellec S, Bellard E, Fournie JJ *et al.* (2011) Human solid tumors contain high endothelial venules: association with T- and B-lymphocyte infiltration and favorable prognosis in breast cancer. *Cancer Res* 71: 5678-5687.

Martinet L, Le Guellec S, Filleron T, Lamant L, Meyer N, Rochaix P *et al.* (2012) High endothelial venules (HEVs) in human melanoma lesions: Major gateways for tumor-infiltrating lymphocytes. *Oncimmunology* 1: 829-839.

Maruyama M, Kobayashi M, Sakai Y, Hiraoka N, Ohya A, Kageyama S *et al.* (2013) Periductal induction of high endothelial venule-like vessels in type 1 autoimmune pancreatitis. *Pancreas* 42: 53-59.

Mitsuoka C, Kawakami-Kimura N, Kasugai-Sawada M, Hiraiwa N, Toda K, Ishida H *et al.*

(1997) Sulfated sialyl Lewis X, the putative L-selectin ligand, detected on endothelial

cells of high endothelial venules by a distinct set of anti-sialyl Lewis X antibodies.

Biochem Biophys Res Commun 230: 546-551.

Naito Y, Saito K, Shiiba K, Ohuchi A, Saigenji K, Nagura H *et al.* (1998) CD8⁺ T cells

infiltrated within cancer cell nests as a prognostic factor in human colorectal cancer.

Cancer Res 58: 3491-3494.

Nakanoma T, Nakamura K, Deguchi N, Fujimoto J, Tazaki H & Hata J. (1992)

Immunohistological analysis of tumour infiltrating lymphocytes in seminoma using

monoclonal antibodies. *Virchows Arch A Pathol Anat Histopathol* 421: 409-413.

Ohya A, Kobayashi M, Sakai Y, Kawashima H, Kageyama S & Nakayama J. (2013)

Lymphocyte recruitment via high endothelial venules in lymphoid stroma of Warthin's

tumour. *Pathology* 45: 150-154.

Paavonen T & Renkonen R. (1992) Selective expression of sialyl-Lewis x and Lewis a

epitopes, putative ligands for L-selectin, on peripheral lymph-node high endothelial

venules. *Am J Pathol* 141: 1259-1264.

Pablos JL, Santiago B, Tsay D, Singer MS, Palao G, Galindo M *et al.* (2005) A HEV-restricted

sulfotransferase is expressed in rheumatoid arthritis synovium and is induced by

lymphotoxin- α/β and TNF- α in cultured endothelial cells. *BMC Immunol* 6: 6.

Padros MR, Noli MI & Fainboim L. (1992) Expression of ICAM-1 (CD54) on normal and

leukaemic B cells: implication for the mixed lymphocyte reaction. *Clin Exp Immunol*

88: 329-334.

Pagès F, Berger A, Camus M, Sanchez-Cabo F, Costes A, Molitor R *et al.* (2005) Effector

memory T cells, early metastasis, and survival in colorectal cancer. *N Engl J Med* 353:

2654-2666.

Parker C, Milosevic M, Panzarella T, Banerjee D, Jewett M, Catton C *et al.* (2002) The

prognostic significance of the tumour infiltrating lymphocyte count in stage I

testicular seminoma managed by surveillance. *Eur J Cancer* 38: 2014-2019.

Pober JS, Gimbrone MA Jr, Lapierre LA, Mendrick DL, Fiers W, Rothlein R *et al.* (1986)

Overlapping patterns of activation of human endothelial cells by interleukin 1, tumor

necrosis factor, and immune interferon. *J Immunol* 137: 1893-1896.

Rothlein R, Dustin ML, Marlin SD & Springer TA. (1986) A human intercellular adhesion

molecule (ICAM-1) distinct from LFA-1. *J Immunol* 137: 1270-1274.

Sato E, Olson SH, Ahn J, Bundy B, Nishikawa H, Qian F *et al.* (2005) Intraepithelial CD8⁺

tumor-infiltrating lymphocytes and a high CD8⁺/regulatory T cell ratio are associated

with favorable prognosis in ovarian cancer. *Proc Natl Acad Sci U S A* 102:

18538-18543.

Sawada M, Takada A, Ohwaki I, Takahashi N, Tateno H, Sakamoto J *et al.* (1993) Specific expression of a complex sialyl Lewis X antigen on high endothelial venules of human lymph nodes: possible candidate for L-selectin ligand. *Biochem Biophys Res Commun* 193: 337-347.

Schrama D, thor Straten P, Fischer WH, McLellan AD, Bröcker EB, Reisfeld RA *et al.* (2001) Targeting of lymphotoxin- α to the tumor elicits an efficient immune response associated with induction of peripheral lymphoid-like tissue. *Immunity* 14: 111-121.

Schwartz BR, Wayner EA, Carlos TM, Ochs HD & Harlan JM. (1990) Identification of surface proteins mediating adherence of CD11/CD18-deficient lymphoblastoid cells to cultured human endothelium. *J Clin Invest* 85: 2019-2022.

Shimojo H, Kobayashi M, Kamigaito T, Shimojo Y, Fukuda M & Nakayama J. (2011) Reduced glycosylation of α -dystroglycans on carcinoma cells contributes to formation of highly infiltrative histological patterns in prostate cancer. *Prostate* 71: 1151-1157.

Streeter PR, Rouse BT & Butcher EC. (1988a) Immunohistologic and functional characterization of a vascular addressin involved in lymphocyte homing into peripheral lymph nodes. *J Cell Biol* 107: 1853-1862.

Streeter PR, Berg EL, Rouse BT, Bargatze RF & Butcher EC. (1988b) A tissue-specific endothelial cell molecule involved in lymphocyte homing. *Nature* 331: 41-46.

Suzawa K, Kobayashi M, Sakai Y, Hoshino H, Watanabe M, Harada O *et al.* (2007) Preferential induction of peripheral lymph node addressin on high endothelial venule-like vessels in the active phase of ulcerative colitis. *Am J Gastroenterol* 102: 1499-1509.

Tanaka H, Hori M & Ohki T. (1992) High endothelial venule and immunocompetent cells in typical medullary carcinoma of the breast. *Virchows Arch A Pathol Anat Histopathol* 420: 253-261.

Tanaka H, Saito S, Sasaki H, Arai H, Oki T & Shioya N. (1994) Morphological aspects of LFA-1/ICAM-1 and VLA4/VCAM-1 adhesion pathways in human lymph nodes. *Pathol Int* 44: 268-279.

Uchimura K, Gauguet JM, Singer MS, Tsay D, Kannagi R, Muramatsu T *et al.* (2005) A major class of L-selectin ligands is eliminated in mice deficient in two sulfotransferases expressed in high endothelial venules. *Nat Immunol* 6: 1105-1113.

von der Maase H, Specht L, Jacobsen GK, Jakobsen A, Madsen EL, Pedersen M *et al.* (1993) Surveillance following orchidectomy for stage I seminoma of the testis. *Eur J Cancer*.

29A: 1931-1934.

Wellicome SM, Thornhill MH, Pitzalis C, Thomas DS, Lanchbury JS, Panayi GS *et al.* (1990)

A monoclonal antibody that detects a novel antigen on endothelial cells that is

induced by tumor necrosis factor, IL-1, or lipopolysaccharide. *J Immunol* 144:

2558-2565.

Yeh JC, Hiraoka N, Petryniak B, Nakayama J, Ellies LG, Rabuka D *et al.* (2001) Novel

sulfated lymphocyte homing receptors and their control by a core 1 extension

β 1,3-*N*-acetylglucosaminyltransferase. *Cell* 105: 957-969.

Yoshida R, Nagira M, Kitaura M, Imagawa N, Imai T & Yoshie O. (1998) Secondary

lymphoid-tissue chemokine is a functional ligand for the CC chemokine receptor

CCR7. *J Biol Chem* 273: 7118-7122.

Zhang L, Conejo-Garcia JR, Katsaros D, Gimotty PA, Massobrio M, Regnani G *et al.* (2003)

Intratumoral T cells, recurrence, and survival in epithelial ovarian cancer. *N Engl J*

Med 348: 203-213.

FIGURE LEGENDS

Figure 1

Histology of HEV-like vessels in seminoma. H & E staining (left panels) shows that venules composed of plump endothelial cells (green dotted line) are found in lymphocyte aggregates among tumor epithelial cell nests. These HEV-like vessels are decorated with MECA-79 (middle panels) and HECA-452 (right panels). HECA-452⁺ mononuclear cells around HEV-like vessels are macrophages. Bar = 100 μm for upper panels, 20 μm for lower panels.

Figure 2

E-selectin•IgM chimera *in vitro* binding assay. The E-selectin•IgM chimera binds to the luminal surface of HEV-like vessels in the presence of calcium (left panel). Sporadic mononuclear cells to which E-selectin•IgM chimera binds are macrophages. Binding is completely abolished in the presence of EDTA (right panel). Bar = 50 μm for upper panels, 20 μm for lower panels.

Figure 3

Double immunofluorescence of HEV-like vessels in seminoma. MECA-79⁺ (green) HEV-like vessels are also ICAM-1-positive (red), as shown by yellow signals in merged image (upper panels). ICAM-1-positive/MECA-79-negative cells around HEV-like vessels

are lymphocytes. VCAM-1 and MAdCAM-1 are not detected on HEV-like vessels in seminoma. Bar = 50 μm .

Figure 4

Triple immunostaining of MECA-79⁺ HEV-like vessels (brown), CD3⁺ T cells (blue), and CD20/CD79 α ⁺ B cells (red). (A) Most TILs in seminoma consist of T cells rather than B cells. (B) HEV-like vessels are observed in the T-cell zone of lymphoid follicles. (C) Both T and B cells attach to the luminal surface of HEV-like vessels. Bar = 500 μm for A, 50 μm for B, and 20 μm for C.

Figure 5

The mean number of CD3⁺ T cells, CD20/79 α ⁺ B cells, or CD8⁺ CTLs per HEV-like vessel. CD3⁺ T cells and CD20/79 α ⁺ B cells attached to the luminal surface of HEV-like vessels were counted in a single section, while CD8⁺ CTLs were counted on an adjacent section. From those numbers the mean number of each lymphocyte subset per vessel was calculated. The number of CD3⁺ T cells exceeds that of B cells, an observation compatible with the presence of TILs in seminoma. By contrast, only a few CD8⁺ CTLs attach to vessels, despite their

predominant infiltration of seminoma. Data are presented as means \pm SD ($n = 24$).

Figure 6

Double immunofluorescence for CD8 (green) and CD3 (red) in TILs from seminoma. Most CD3⁺ T cells infiltrating seminoma are CD8⁺ CTLs. Bar = 50 μ m.

Figure 7

Double immunostaining for CD8⁺ CTLs (purple) and either MECA-79⁺ HEV-like vessels (A) or Ki-67 (B) (both brown). Large numbers of CTLs infiltrate at extravascular sites, but only a small number of CTLs attach to the luminal surface of HEV-like vessels (A). Large numbers of tumor-infiltrating CTLs are proliferating, based on Ki-67 positivity (arrows) (B). Bar = 50 μ m.

Table 1

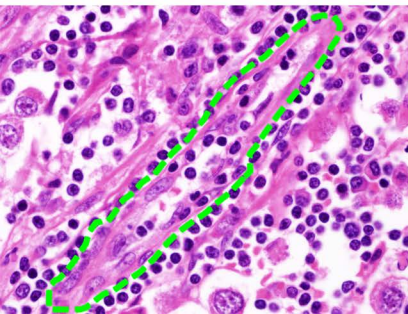
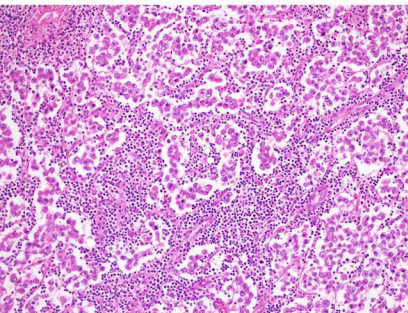
Clinical characteristics of 26 patients with seminoma

Age (years)	
Mean \pm SD	39.5 \pm 10.8
Range	27-63
<hr/>	
	Number (%)
Affected site	
Left	16 (61.5%)
Right	10 (38.5%)
Primary tumor (pT classification*)	
pT1	16 (61.5%)
pT2	6 (23.1%)
pT3/pT4	4 (15.4%)
Regional lymph node metastasis	
Negative (N0)	18 (69.2%)
Positive (N1/N2/N3)	8 (30.8%)
Serum tumor markers (S classification*)	
S0	12 (46.2%)
S1	7 (26.9%)
S2	7 (26.9%)
S3	0 (0%)
Stage*	
Stage IA/IB/IS	18 (69.2%)
Stage IIA/IIB/IIC	4 (15.4%)
Stage IIIA/IIIB/IIIC	4 (15.4%)

*T and S classification and staging are based on the 7th edition of TNM classification

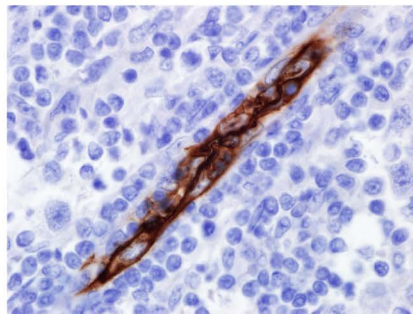
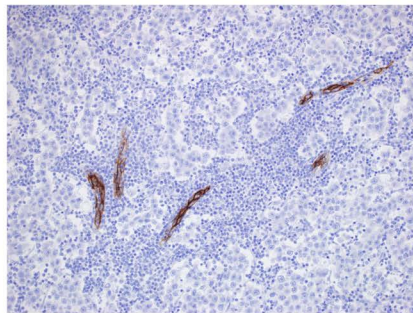
developed by Union for International Cancer Control (UICC).

H & E

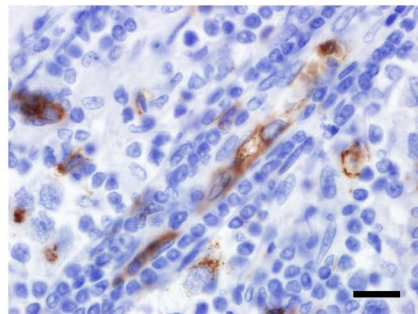
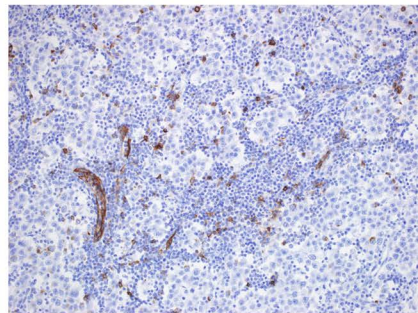


Immunohistochemistry

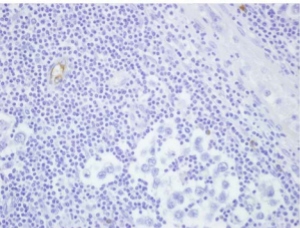
MECA-79



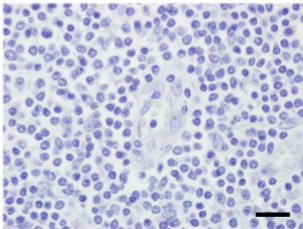
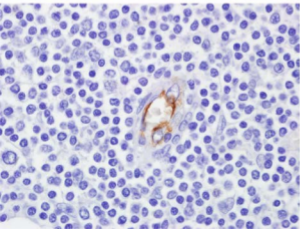
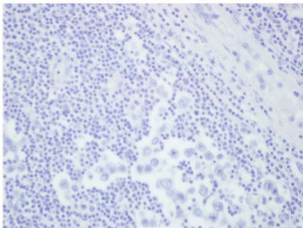
HECA-452



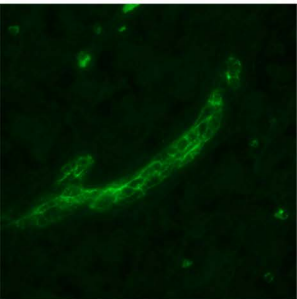
without EDTA



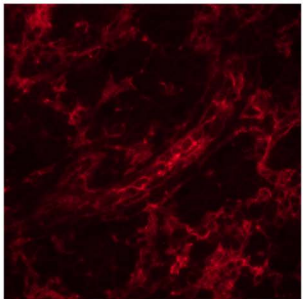
with EDTA



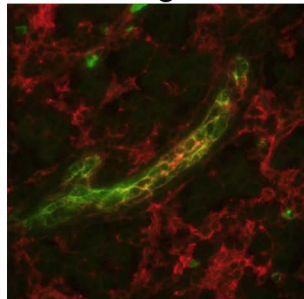
MECA-79



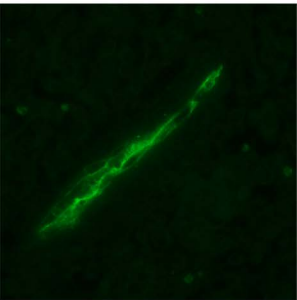
ICAM-1



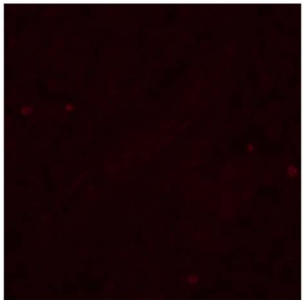
Merged



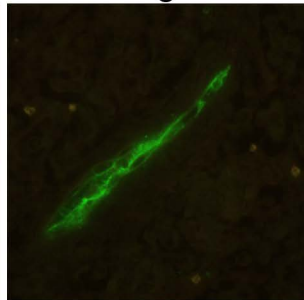
MECA-79



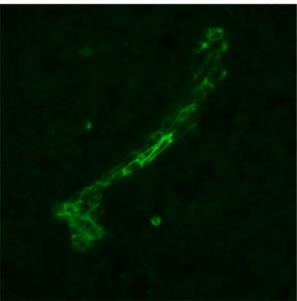
VCAM-1



Merged



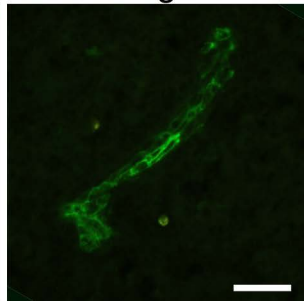
MECA-79

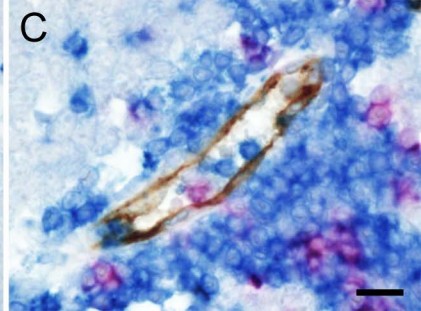
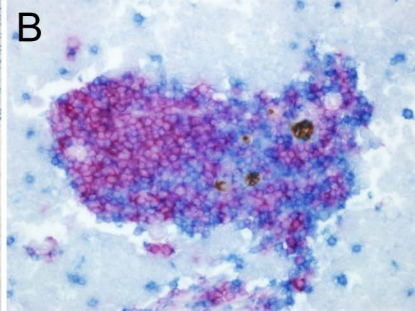
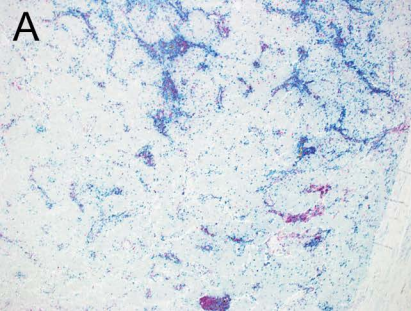


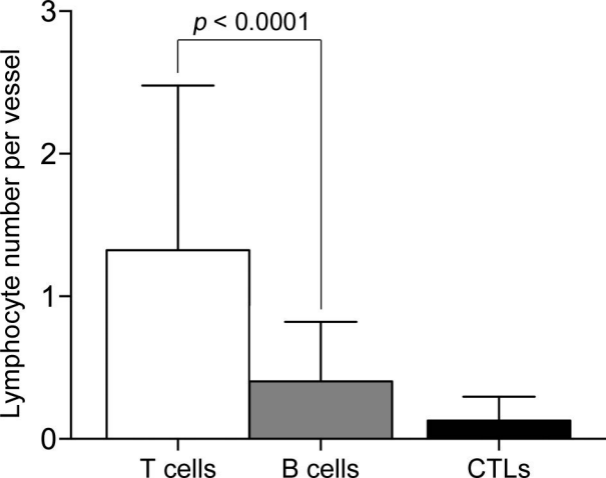
MAdCAM-1



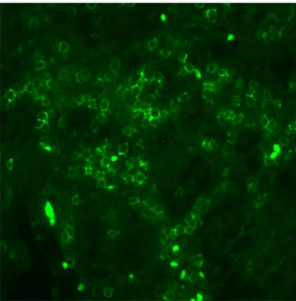
Merged



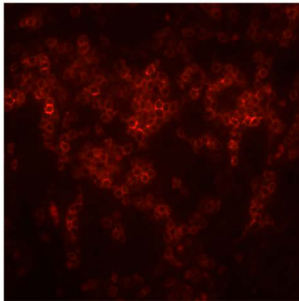




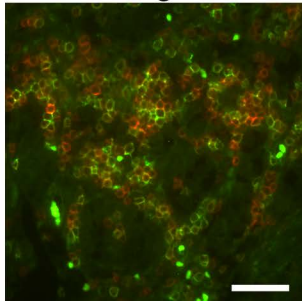
CD8



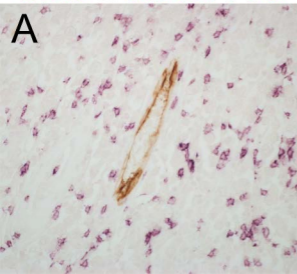
CD3



Merged



CD8 & MECA-79



CD8 & Ki-67

